Numerical study of multi-dimensional effects on the transition to detonation from subsonic self-ignition waves propagating at constant speed

Said Taileb[§], Emmeline Rougon[†], Ashwin Chinnayya[†], Vincent Robin[†]
[†] Institut PPRIME - UPR 3346 - CNRS - ISAE-ENSMA - Université de Poitiers, France
[§]Aix Marseille Univ, CNRS, Centrale Marseille, M2P2 Marseille, France

1 Introduction

The transition from a subsonic deflagration to a supersonic detonation wave (DDT) can be achieved through different scenarios, which involve interactions of flames with shocks, boundary layers, instabilities or turbulence. This well-known combustion problem has been extensively studied over the past decades (see for example the review paper [1] or more recent studies [2–4]). This has led to an abundant literature, due to the physics of which is extremely rich, and of which understanding can lead to potential improvements to industrial applications. A better understanding of the transition is necessary either to control its initiation for optimization of future propulsive systems such as rotating detonation engines, either to avoid detonation, which is very destructive. More recently, in the context of a rapid reduction of greenhouse gas emissions, the expected increase in the use of hydrogen also requires more studies in the context of safety hazards. The underlying physical mechanisms are also responsible for engine knock, explosions when handling and storing energetic materials, and also for non-terrestrial phenomenon, such as, explosions of Ia type supernova.

Detonation initiation can be achieved in three different ways [5]. First, the strong ignition is the result of an initial shock wave strong enough to trigger chemical reactions. Second, the weak ignition is the result of self-ignition mechanisms through a gradient of temperature or composition. The third way is deflagration to detonation transition (DDT): a flame propagating by heat and species diffusion mechanism at constant speed, initially laminar, increases its surface through instabilities or interactions with turbulence or boundary layers until the compression waves coalesce to become a precursor shock.

The scenario studied in this article exhibits both the characteristics of weak ignition and DDT. First, a sharp gradient of temperature is initially set in the fresh gases for the spontaneous wave to be subsonic. Then, the initial reactive wave area is set sufficiently large to promote transition. The low speed of the reactive wave produces, in a 1-D domain, weak compression waves that have negligible effects on the fresh gases conditions. In addition, the wave speed is large enough ($10\,\mathrm{m/s}$ to $50\,\mathrm{m/s}$) to neglect dissipative effects. Moreover, the carefully defined initial profile of temperature allows the wave speed to be constant and its value to be perfectly controlled. Accordingly, the initial gradient of reactivity [6], i.e. gradient of ignition delay time, is kept constant. The first originality of the present study lies in this specific initial condition. Indeed, previous studies of such reactive waves considered a constant temperature gradient [7] or a gradient resulting from energy deposition mechanism [8] where the 1-D

Correspondence to: vincent.robin@isae-ensma.fr

compression waves modify the fresh gas conditions [9]. As a consequence, the reactive waves were either accelerating or decelerating but were never at constant speed, as proposed here.

At first, subsonic 1-D cases are considered with different initial velocities for the reactive wave. Then, for conditions in which the 1-D configuration cannot induce any transition, 2-D and 3-D configurations, which constitute the second originality of the present study are shown to exhibit potential acceleration and transition to detonation. There is no initial turbulence in the domain, but a specific shape of the reactive wave is imposed, mimicking an increase of the reactive wave area. Eventually, the results highlight the transition scenario from subsonic waves to detonation.

2 Equations solved and numerical methods

The flow is described by the compressible reactive Euler equation with a single step chemistry for an ideal gas. An in-house code RESIDENT (REcycling mesh SImulations of DEtoNaTions) is used to solve the governing equations. Further description of the numerical methodology can be found in [10, 11]. Briefly, a classical time-operator splitting method along with directional splitting is used to couple the hydrodynamics and chemistry. To reduce dissipation, a 9^{th} Monotonicity Preserving interpolation is used to reconstruct the characteristics variables at the cell boundary [12]. A HLLC Riemann solver is used to calculate the time-averaged conservative fluxes at the cell interfaces [13]. A third-order Runge-Kutta method is employed for the temporal resolution. The parallelization of the code is achieved through a domain decomposition method (MPI). Typical computations are performed on 240 processors, with a cost of about 4800 CPU scalar hours.

3 Initial conditions from 1-D low-Mach spontaneous waves

The dimensions of the Cartesian computational domains are $L_x = 300\,\text{mm}$, $L_y = 10\,\text{mm}$ and for the 2-D and 3-D cases $L_z = 0.1\,\text{mm}$ and $L_z = 10\,\text{mm}$, respectively. The cell size is $\Delta = 0.1\,\text{mm}$. All boundaries are slip walls except the $x = L_x$-plane which is transmissive. Similar conclusions have been obtained using transmissive boundaries although the flow slightly differs. The domains are initially filled with partially burnt gases, see Fig. 1, obtained from the pressure constant combustion of stoichiometric hydrogen/air mixture at high pressure (16 atm). A strong temperature gradient is set to obtain the propagation of the ignition front towards the reactive mixture. The 2-D initial field is obtained from the same 1-D profile that is applied normally to the iso-surface corresponding to the initial flame front position. The geometry of the surface corresponds to the interaction of two plane flame fronts for the 2-D case, as described on Fig. 1. The 3-D case is a cone obtained from the revolution of the 2-D case.

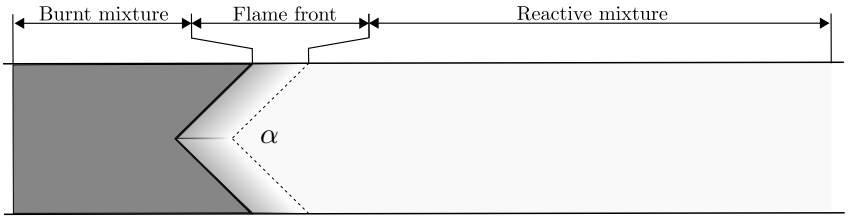

Figure 1: Initial flame shape of the 2-D case corresponding to the interaction of two plane fame fronts (angle α) which propagate from the left to the right and initially at constant speed.

The whole procedure to compute the 1-D profile is designed to be valid using a detailed chemical mechanism but, for the sake of clarity, a global single-step reaction of hydrogen combustion has been considered $2\,H_2 + O_2 \longrightarrow 2\,H_2O$. The chemical reaction rate $\dot{\omega}$ is an Arrhenius law: $\dot{\omega} = K \exp\left(-E_a/RT\right)$.

The reduced activation energy is E_a/RT_0=35 (T_0=300 K) and the pre-exponential factor $K = 2.6 \times 10^8\,\mathrm{s}^{-1}$ has been calibrated to obtain realistic ignition delay times comparable with those obtained using a detailed chemical mechanism in the high temperature range [14]. The ratio of specific heat and the heat release are $\gamma = 1.35$ and $q/RT_0 = 816.3$, respectively. From preliminary 0-D constant pressure computations using the Cantera library, a database of time evolution quantities, $\rho(t, T_u)$, $Y(t, T_u)$, $T(t, T_u)$, see Fig. 2-left, is first created for a large range of fresh gas temperature values T_u. The ignition delay times $\tau_i(T_u)$ for each value of T_u are then stored.

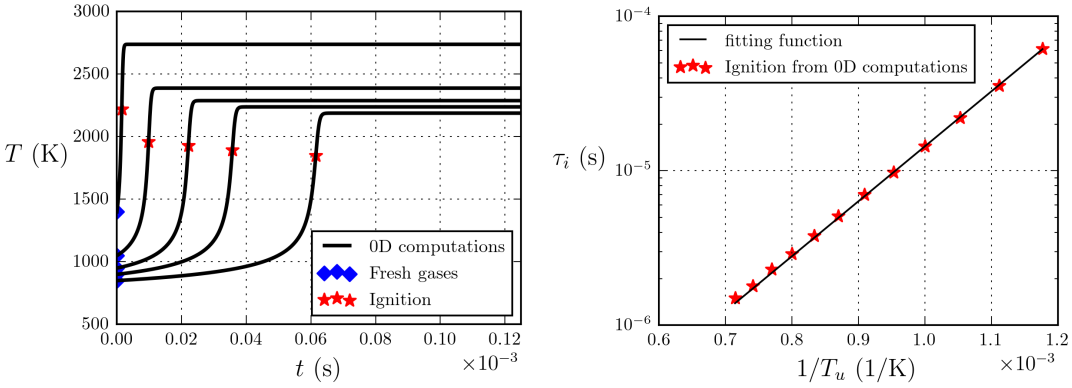

Figure 2: **Left**: Time evolution of the temperature (solid lines) for different values of fresh gas temperature T_u (blue diamond) obtained from 0-D computations. The red stars represent the self-ignition delay definition, determined from the maximum gradient. **Right**: Self-ignition delay time as a function of T_u (red stars) and the corresponding fitting function (solid line).

A fitting function for $\tau_i(T_u)$, see Fig. 2-right, is introduced:

$$\tau_i(T_u) = b \exp\left(\frac{a}{T_u}\right) \quad \text{with} \quad a = 8196.2\,\mathrm{K}, \quad b = 3.9830 \times 10^{-9}\,\mathrm{s} \tag{1}$$

Based on the Zel'dovich gradient theory [6], the propagation velocity S_n in the normal direction n of the reactive wave is considered constant and gives, after integration, the ignition delay time along the normal direction:

$$S_n = \left(\frac{d\tau_i}{dn}\right)^{-1} \qquad \rightarrow \qquad \tau_i(x_n) = \frac{x_n - x_{mr}}{S_n} + \tau_{mr} \tag{2}$$

The ignition delay time of the most reactive mixture, τ_{mr} is located at $x_n = x_{mr}$. This location corresponds to the first ignited point. The inverse of Eq. (1), i.e. $T_u(\tau_i) = a/\log(\tau_i/b)$, combined with Eq. (2) gives the fresh gas temperature profile along the normal direction leading to a constant ignition front speed S_n:

$$T_u(x_n) = a/\log\left(\frac{x_n - x_{mr}}{S_n b} + \frac{\tau_{mr}}{b}\right), \tag{3}$$

The dashed line of Fig. 3-left shows an example of the fresh gas temperature profile for $\tau_{mr} = 10\,\mu\mathrm{s}$ and $S_n = 60\,\mathrm{m/s}$. Thus, a $10\,\mu\mathrm{s}$ delay is necessary for the front to enter the domain and propagates at a constant velocity of $60\,\mathrm{m/s}$, see the solid line of Fig. 3-left which shows the temperature profile after the front has traveled about twenty millimeters. Then, this profile of partially burnt gas is taken as an initial condition with the whole set of equations in the numerical code. As expected, the computation with RESIDENT of this 1-D case, yields a reactive wave propagating at a constant velocity (see Figure 3-right). A compression wave is also generated, amplitude of which is negligible. The compression and reaction waves speed are constant and are about $600\,\mathrm{m/s}$ (sound speed) and $60\,\mathrm{m/s}$, respectively.

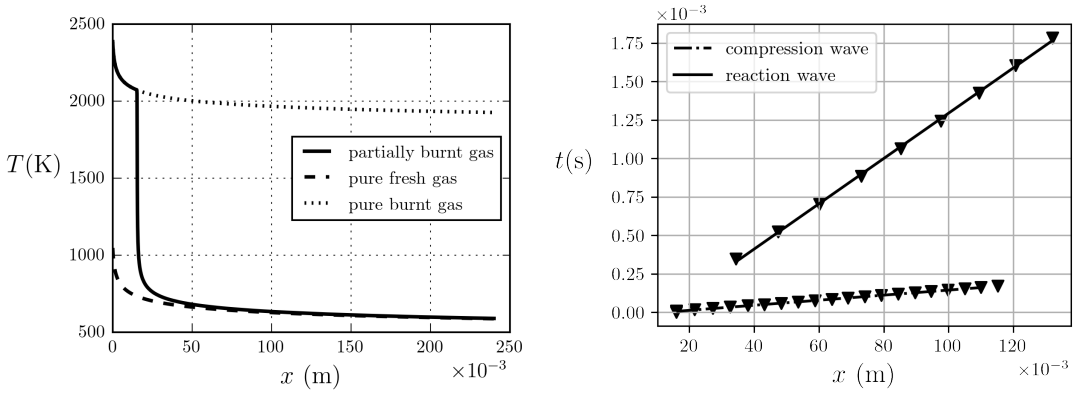

Figure 3: **Left**: Fresh gas temperature profile leading to a constant speed self-ignition wave (dashed line) and corresponding fully burnt gas (dotted line). The solid line is an intermediate case where the self-ignition wave is inside the domain. **Right**: $x-t$ diagram corresponding to the maximum of pressure gradient obtained from the 1-D RESIDENT computation.

Eventually, this initial 1-D profile is also used to set the initial conditions of multi-dimensional simulations. The reaction wave speed S_n is taken hereafter to be $40\,\mathrm{m/s}$. The angle between the initial plane flame fronts (2-D) is $\alpha = 10°$, see Fig. 1. The 1-D-profile is applied on the flame-normal direction to fill the initial 2-D and 3-D domains.

4 Transition scenario

Figure 4 presents 3-D results corresponding to six time steps of the transition to detonation and showing for each time step the numerical Schlieren (Sch), the Mach field and the iso-surface of fuel mass fraction $Y = 1/2$ colored with the temperature field. The Mach field has been defined in the frame of the pressure waves that propagate approximately at $630\,\mathrm{m/s}$. During the subsonic transients ($t_1 = 84.4\,\mu\mathrm{s}$) of the cone-shaped front, the fresh gases converge to the center of the cone-shaped. The form of the reactive wave is that of a tulip, with a stem. This tulip-shaped front is due to a hydrodynamic mechanism similar to what happens in laminar flames. The global flame surface initially greater than that of the 1-D case, increases and is also large enough to generate a significant compression in fresh gases. The flame is observed to become more flat, except at the center, decreasing then significantly its surface. The convergence of the flow at the center induces that the center of the flame is pushed away, towards the burned side, where the gases are not yet affected by compression. The stem of the tulip therefore grows to finally create a fresh gas pocket in the burnt gas side ($t_2 = 85.2\,\mu\mathrm{s}$). The stem has dissociated from the flower, and a sudden acceleration at its center occurs, creating a hot spot ($t_3 = 89.1\,\mu\mathrm{s}$). Downstream of the reactive wave position, a first shock appears near the center when the flame has reached sonic conditions between t_3 and $t_4 = 93\,\mu\mathrm{s}$. Moreover, interaction of these pressure waves coalesce into Mach stems at the front. A complex shock wave structure also develops. The reaction front quickly becomes coupled to the shock at $t_5 = 96\,\mu\mathrm{s}$. Further wave instabilities propagate on the flame surface, continuously interacting with the domain boundaries. The last time step $t_6 = 103\,\mu\mathrm{s}$ clearly shows the development of a cellular detonation.

Eventually, these results describe a potential scenario for the acceleration of a subsonic reactive wave to detonation that are due to multi-dimensional effects. From an increased initial flame surface as compared to the 1-D case, a combination of hydrodynamic effect, which increases the flame surface at first, and compression waves, accelerate the front. The reactive wave surface then decreases sharply, and a

complex wave structure appears, due to the coupling of the reaction zone to the precursor shock, that develops further to a cellular detonation structure.

Acknowledgements
The computations were performed using HPC resources from GENCI-CINES (Grant 2020-A0092B07735). This work was supported by the CPER FEDER Project of Région Nouvelle Aquitaine. This work pertains to the French Government program "Investissements d'Avenir" (EUR INTREE, reference ANR-18-EURE-0010)

References

[1] Oran ES, Gamezo VN (2007) Origins of the deflagration-to-detonation transition in gas-phase combustion. Combustion and Flame 148: 1-2, 4–47.

[2] Yang H, Radulescu MI (2021) Enhanced ddt mechanism from shock-flame interactions in thin channels. Proceedings of the Combustion Institute 38: 3, 3481–3495.

[3] Ballossier Y, Virot F, Melguizo-Gavilanes J (2021) Strange wave formation and detonation onset in narrow channels. Journal of Loss Prevention in the Process Industries 72, 104535.

[4] Towery CA, Poludnenko AY, Hamlington PE (2020) Detonation initiation by compressible turbulence thermodynamic fluctuations. Combustion and Flame 213, 172–183.

[5] Poludnenko AY, Chambers J, Ahmed K, Gamezo VN, Taylor BD (2019) A unified mechanism for unconfined deflagration-to-detonation transition in terrestrial chemical systems and type ia supernovae. Science 366: 6465.

[6] Zeldovich Y (1980) Regime classification of an exothermic reaction with nonuniform initial conditions. Combustion and Flame 39: 2, 211–214.

[7] Kapila A, Schwendeman D, Quirk J, Hawa T (2002) Mechanisms of detonation formation due to a temperature gradient. Combustion Theory and Modelling 6: 4, 553.

[8] Liberman M, Ivanov M, Kiverin A (2015) Effects of thermal radiation heat transfer on flame acceleration and transition to detonation in particle-cloud hydrogen flames. Journal of Loss Prevention in the Process Industries 38, 176–186.

[9] Deshaies B, Joulin G (1989) Flame-speed sensitivity to temperature changes and the deflagration-to-detonation transition. Combustion and flame 77: 2, 201–212.

[10] Taileb S, Melguizo-Gavilanes J, Chinnayya A (2020) Influence of the chemical modeling on the quenching limits of gaseous detonation waves confined by an inert layer. Combustion and Flame 218, 247–259.

[11] Reynaud M, Virot F, Chinnayya A (2017) A computational study of the interaction of gaseous detonations with a compressible layer. Physics of Fluids 29: 5, 056101.

[12] Suresh A, Huynh HT (1997) Accurate monotonicity-preserving schemes with Runge–Kutta time stepping. Journal of Computational Physics 136: 1, 83–99.

[13] Toro EF, Spruce M, Speares W (1994) Restoration of the contact surface in the HLL-riemann solver. Shock Waves 4: 1, 25–34.

[14] Mével R, Sabard J, Lei J, Chaumeix N (2016) Fundamental combustion properties of oxygen enriched hydrogen/air mixtures relevant to safety analysis: Experimental and simulation study. international journal of hydrogen energy 41: 16, 6905–6916.

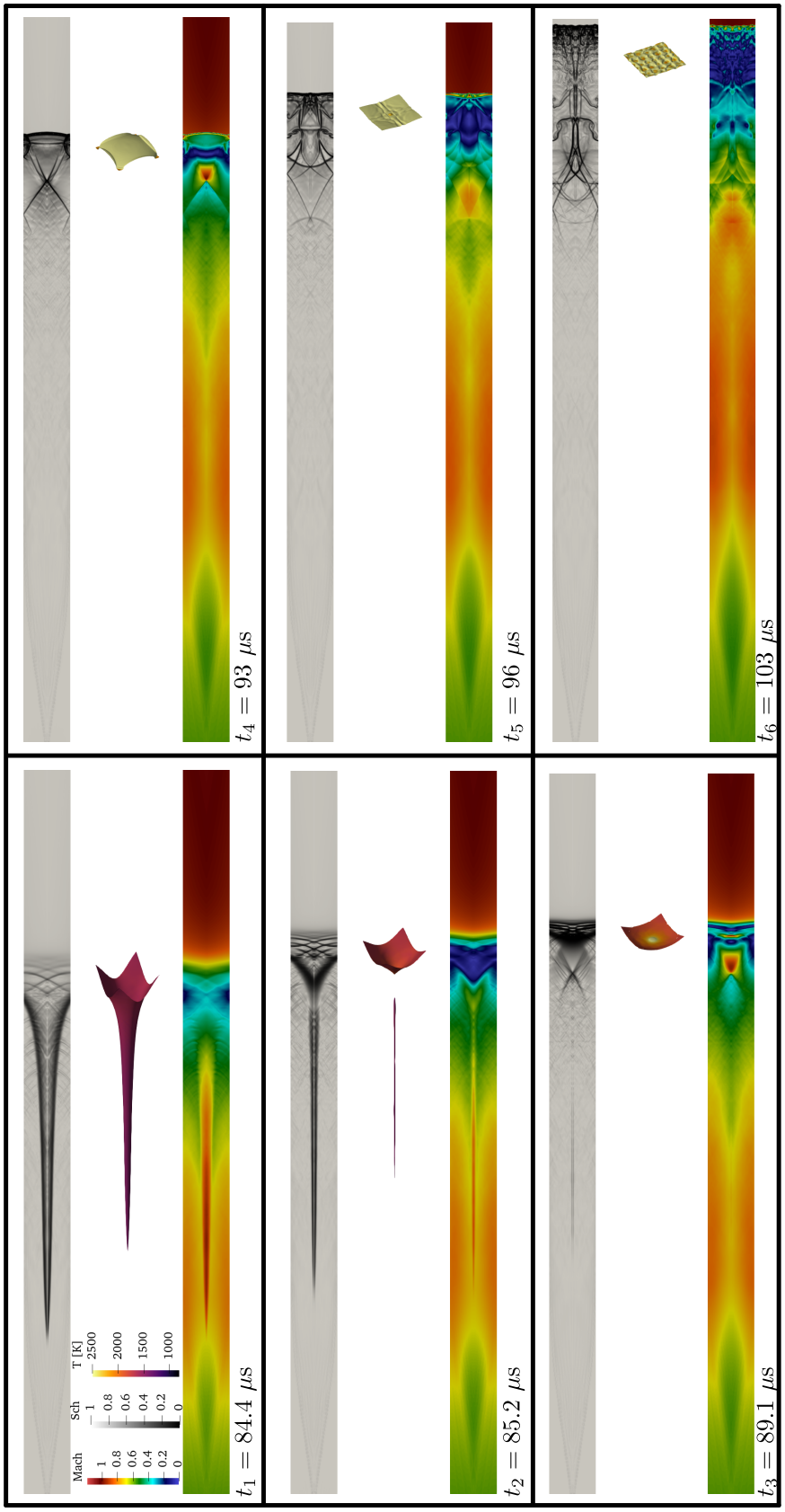

Figure 4: 3-D results obtained with RESIDENT corresponding to six time steps: 84.4 µs, 85.2 µs, 89.1 µs, 93 µs, 96 µs, 103 µs.